chemistry proceedings

MDPI

Proceeding Paper

Pyrene-4,5,9,10-Tetrachalcogenone Derivatives: A Computational Study on Their Potential Use as Materials for Batteries †

M. Pilar Vázquez-Tato [1], Francisco Meijide [2], Francisco Fraga [3], José Vázquez Tato [2] and Julio A. Seijas [1,*]

[1] Departamento de Química Orgánica, Facultade de Ciencias, Universidade de Santiago de Compostela—Campus Terra, 27080 Lugo, Spain
[2] Departamento de Química Física, Facultade de Ciencias, Universidade de Santiago de Compostela—Campus Terra, 27080 Lugo, Spain
[3] Departamento de Física Aplicada, Facultade de Ciencias, Universidade de Santiago de Compostela—Campus Terra, 27080 Lugo, Spain
* Correspondence: julioa.seijas@usc.es
† Presented at the 26th International Electronic Conference on Synthetic Organic Chemistry, 15–30 November 2022; Available online: https://sciforum.net/event/ecsoc-26.

Abstract: Polycyclic aromatic hydrocarbons are versatile building blocks for conjugated materials and can be applied in molecular electronics. Pyrenes are known as the best organic chromophores, and pyrene itself is known as an electron donor. Likewise, quinones are promising electrode materials for lithium-ion batteries. The calculations were performed for pyrene-4,5,9,10-tetrathione, pyrene-4,5,9,10-tetraselenone and pyrene-4,5,9,10-tetratellurone, and the results were compared with those for pyrene-4,5,9,10-tetraone. The results obtained indicate that the sulfur derivative is a suitable candidate for further experimental studies since, although selenium and tellurium compounds present better prospects than 4,5,9,10-tetraoxopyrene, they require the improvement of available synthetic techniques or even the discovery of new ones.

Keywords: pyrene-4,5,9,10-tetrachalcogenones; battery; organic electrode; DFT; reduction potential; sulfur; selenium; tellurium; cathode

Citation: Vázquez-Tato, M.P.; Meijide, F.; Fraga, F.; Tato, J.V.; Seijas, J.A. Pyrene-4,5,9,10-Tetrachalcogenone Derivatives: A Computational Study on Their Potential Use as Materials for Batteries. *Chem. Proc.* **2022**, *12*, 76. https://doi.org/10.3390/ecsoc-26-13554

Academic Editor: Enrique Cabaleiro Lago

Published: 14 November 2022

1. Introduction

Powered by the rising demand for large-scale electrochemical energy storage devices such as smart grids and electric vehicles, low-cost batteries with high energy density have become a major interest among sustainable energy research [1]. Within this field, organic electrode materials have become rather promising candidates for lithium-ion batteries, since organic constituents usually have the advantages of higher recyclability and easier synthesis against inorganic compounds [2]. The lithium storage mechanism of organic carbonyl compounds relies on the redox reactions of the oxygen atom on the carbonyl group, which is able to undergo a reversible one-electron reduction to generate a radical anion that combines with lithium ions [3]. Among other candidates, quinone derivatives have been studied experimentally as promising organic electrode materials, given that the reversible redox reactions occur between Li atoms and the carbonyl group. While discharging, the oxygen atom on each carbonyl group obtains an electron along with a lithium ion to form a lithium enol salt. While charging, lithium ions are released with electrons from the enol salts and return to the carbonyl groups. The reversible insertion and extraction of the lithium ions are achieved through the conversion between the carbonyl and enol structures. The main merits of the quinone compound cathode materials are their great theoretical capacity (902 mA h g^{-1}) and high redox potential (3.0 V vs. Li/Li^+) [3]; in particular, pyrene-4,5,9,10-tetraketone (**1**, PTO) has a capacity of 409 mA h g^{-1} [4–6] and has been studied in depth both experimentally and theoretically [7]. This communication presents the theoretical study of

reduction potential for chalcogen analogs of PTO, namely pyrene-4,5,9,10-tetrathione (**2**, PTS), pyrene-4,5,9,10-tetraselenone (**3**, PTSe) and pyrene-4,5,9,10-tetratellurone (**4**, PTTe) and compares the results with those of pyrene-4,5,9,10-tetraone (Figure 1).

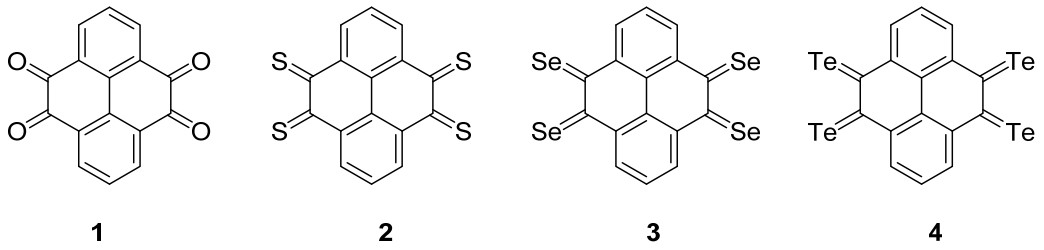

Figure 1. Pyrene-4,5,9,10-tetraketone (**1**, PTO), pyrene-4,5,9,10-tetrathione (**2**, PTS), pyrene-4,5,9,10-tetraselenone (**3**, PTSe) and pyrene-4,5,9,10-tetratellurone (**4**, PTTe).

2. Results and Discussion

Density functional theory (DFT) calculations were performed with the Gaussian 16 program package [8] at the B3LYP/LANL2DZ level. For the solution calculations, dimethyl sulfoxide (DMSO) was chosen (using a polarizable continuum model), due to its low toxicity and because it is a non-hazardous solvent that can solubilize a vast variety of organic compounds [9]. The vibrational frequency analysis was performed at the same level of theory and the obtained positive frequencies confirmed that the optimized geometries were found at the real minima on the potential energy surfaces.

Electron transfer during an electrochemical process leads to the reduction/oxidation of the compound. The redox ability of the compound can be quantitatively described by the redox potential. Consequently, the performance of organic electrical devices is highly dependent on the oxidation potential (E_{OX}) and the reduction potential (E_{RED}) of the used materials. These potentials govern the materials' capability to capture (or inject) holes and electrons, respectively, in the devices.

The thermodynamic cycle for the Gibbs free energy of the oxidation and reduction reaction of the molecule (A) is displayed in Scheme 1 [10].

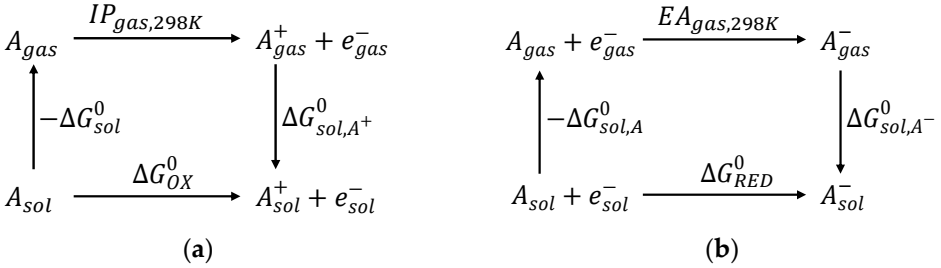

Scheme 1. Thermodynamic cycle for the Gibbs free energy of the (**a**) oxidation and (**b**) reduction reactions of a molecule.

The ΔG_{sol} is evaluated as the electronic energy difference of the molecule in the gas phase and the solvated one using the equilibrium geometry obtained in vacuum.

To estimate the charge transfer properties, the Marcus theory was used, according to which the reorganization energy (λ) has both intra- and intermolecular contributions. The former reflects the deformation of molecular geometry in order to accommodate charge transfer; the latter reflects the electronic polarization of the surrounding molecules, being much smaller than the intramolecular one, and is usually neglected. The intramolecular reorganization energy can be evaluated either from the adiabatic potential energy surfaces

or from normal mode analysis [11]. In this method, the hole and electron reorganization energies ($\lambda_{h/e}$) are defined by the following equation:

$$\lambda_{h/e} = \lambda^1 + \lambda^2$$

$$\lambda^1 = E_N(Q_{h/e}) - E_N(Q_N)$$

$$\lambda^2 = E_{h/e}(Q_N) - E_{h/e}(Q_{h/e})$$

where $E_N(Q_N)$ and $E_{h/e}(Q_{h/e})$ are the ground-state energies of the optimized neutral and ionic states, respectively, $E_N(Q_{h/e})$ is the energy of the charged molecules at the optimal geometry of the neutral molecules, and $E_{h/e}(Q_N)$ is the energy of the neutral molecules at the optimal ionic geometry.

The adiabatic ionization potential $IP_{(a)}$ and adiabatic electron affinity $EA_{(a)}$ are two important parameters needed to evaluate the oxidation and reduction ability of charged organic molecules. A large $EA_{(a)}$ is beneficial for stabilizing the organic radical anions and decreases the electron injection energy barrier and, hence, is helpful for electron transport [12]. Thus, the corresponding adiabatic IPs and EAs were obtained with the following equations:

$$IP_{(a)} = E_h(Q_h) - E_N(Q_N)$$

$$EA_{(a)} = E_N(Q_N) - E_e(Q_e)$$

In evaluating electron rearrangement energy, the two alternatives are that either the transfer occurs with the motion of one electron, or it occurs simultaneously with several electrons at the same time [13]. Figure 2 describes the adiabatic potential energy surface method, which is used for calculating the reorganization energy for dianion in both cases: through the monoanion with the transfer of one electron in two stages and when two electrons are transferred in a single process.

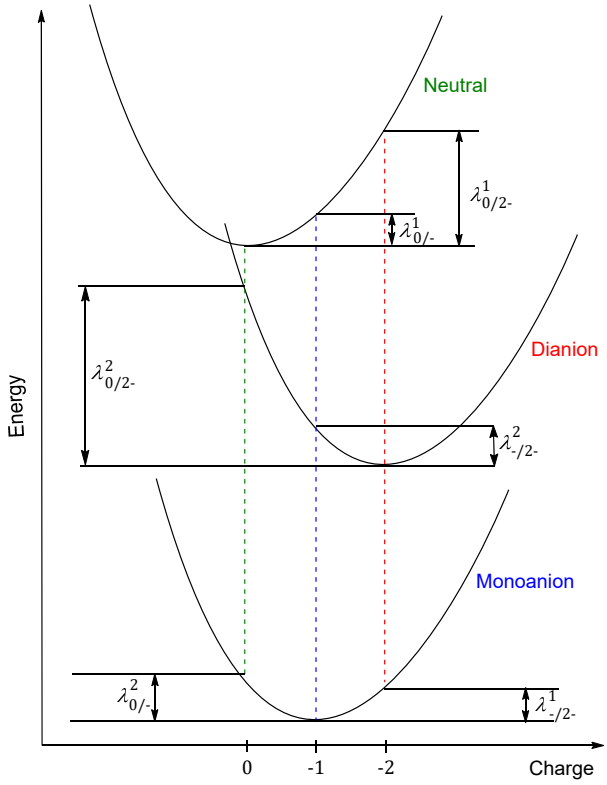

Figure 2. Schematic plot of reorganization energy for electron transfer for compounds PTO, PTS, PTSe and PTTe.

The redox potentials $[Z]^{0/-}$, $[Z]^{0/2-}$, $[Z]^{0/3-}$ and $[Z]^{0/4-}$ of the different species, resulting in the corresponding mono, di, tri and tetra-anion (Scheme 2), were calculated as mentioned above, together with the corresponding electron reorganization energies (λ) to check the feasibility of the reduction process. Lower λ values are related to higher charge carrier mobility (Table 1).

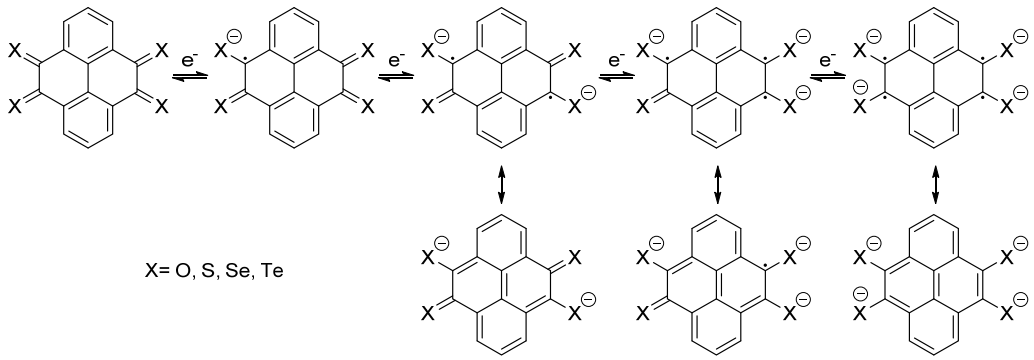

Scheme 2. Electron transfer in redox processes $[Z]^{0/-}$, $[Z]^{0/2-}$, $[Z]^{0/3-}$ and $[Z]^{0/4-}$, and resonance structures of corresponding anions.

Table 1. Reduction potentials and electron reorganization energies for redox processes $[Z]^{0/-}$, $[Z]^{0/2-}$, $[Z]^{0/3-}$ and $[Z]^{0/4-}$(b3lyp/lanl2dz).

Compound	PTO	PTS	PTSe	PTTe
$[Z]^{0/-}$	−4.35	−4.18	−4.17	−6.50
$[Z]^{0/2-}$	−7.55	−9.42	−7.77	−9.69
$[Z]^{0/3-}$	−10.61	−12.91	−11.88	−13.49
$[Z]^{0/4-}$	−12.58	−16.11	−14.96	−16.46
$\lambda_{0/-}$	0.14	2.22	0.87	0.58
$\lambda_{0/2-}$	0.99	3.51	3.13	2.12
$\lambda_{0/3-}$	1.80	4.58	5.39	4.32
$\lambda_{0/4-}$	2.92	8.17	8.70	7.04

The results for $[Z]^{0/-}$ calculation are similar, with lower potentials for PTS and PTSe; only in the case of tellurium was the potential clearly more negative than that of PTS. For the reduction to the $[Z]^{0/2-}$ species, compound PTS resulted in −9.42 V, demonstrating an approximately −2 V difference between oxygen and selenium compounds and similar to the value of the compound with tellurium atoms. The same trend was found for the potentials $[Z]^{0/3-}$ and $[Z]^{0/4-}$. Generally, lower λ values are related to higher charge carrier mobility, and in the present study, those of PTS, PTSe and PTTe were greater than that of PTO.

Figure 3 shows the energy of the orbitals in the outer shell for PTO, PTS, PTSe and PTTe, indicating for each compound the HOMO, LUMO and LUMO + 1 of the neutral species, where electrons gained throughout the reduction process were located. The energy difference between the orbitals of each charged species was similar for PTS, PTSe and PTTe, with the difference between HOMO and LUMO being higher for the PTO than the other compounds.

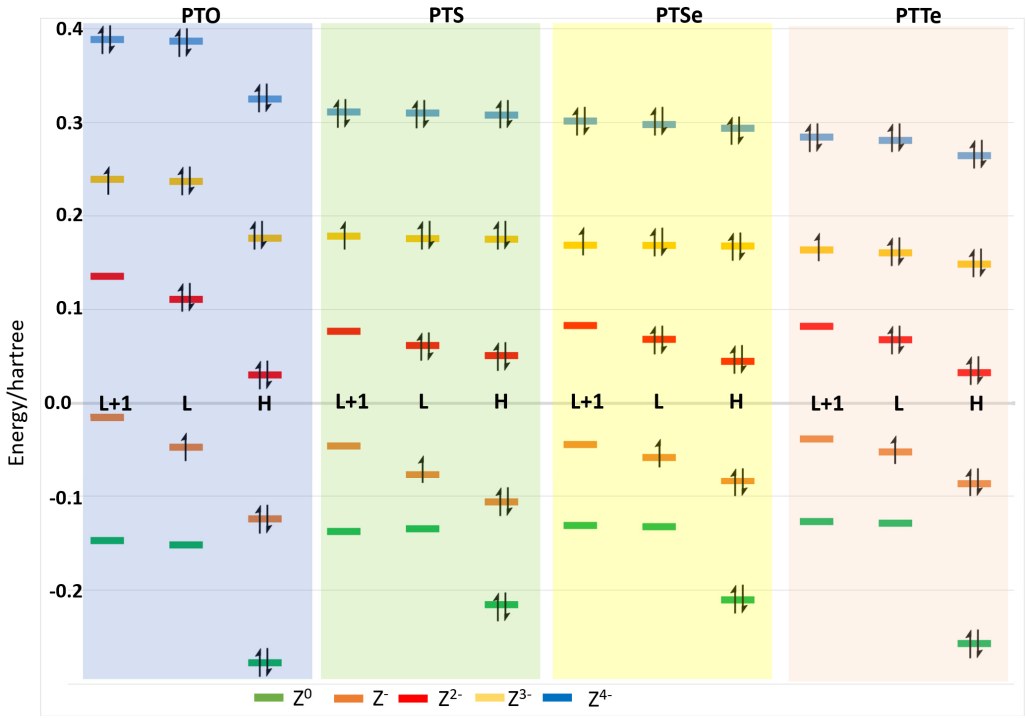

Figure 3. Schematic plot of the orbitals energy HOMO (H), LUMO (L) and LUMO + 1 (L + 1) for neutral compounds PTO, PTS, PTSe and PTTe, and charged species −1, −2, −3 and −4. In each orbital, the occupancy is shown.

The values for PTS indicated in Table 2 show, as mentioned above, a value for $\lambda_{(0/-)}$ that is high when compared to those obtained for the other compounds. There is at least one additional possible geometry (Figure 4b), which is not as flat as the previous one (Figure 4a), with the sulfur atoms being out of the plane of the rings, which also meets the requirement of lacking vibrations with a negative value and therefore corresponds to a minimum on the potential energy surface. The neutral non-planar conformation of PTS was 2.32 Kcal/mol more stable in vacuum and 3.70 Kcal/mol in DMSO as a solvent.

Table 2. Reduction potentials and electron reorganization energies for redox processes $[Z]^{0/-}$, $[Z]^{0/2-}$, $[Z]^{0/3-}$ and $[Z]^{0/4-}$(b3lyp/lanl2dz) for PTS and its conformer with sulfur atoms out of the plane of the carbon skeleton.

Compound	PTS	Out-of-Plane PTS
$[Z]^{0/-}$	−4.18	−4.59
$[Z]^{0/2-}$	−9.42	−8.54
$[Z]^{0/3-}$	−12.91	−12.61
$[Z]^{0/4-}$	−16.11	−15.91
$\lambda_{0/-}$	2.22	0.26
$\lambda_{0/2-}$	3.51	0.91
$\lambda_{0/3-}$	4.58	1.92
$\lambda_{0/4-}$	8.17	3.30

This out-of-plane structure for PTS (Figure 4b) was used to calculate the reduction potentials in order to obtain the corresponding anions ($[Z]^{0/-}$, $[Z]^{0/2-}$, $[Z]^{0/3-}$, $[Z]^{0/4-}$), as well as their electronic rearrangement energies (λ). The new values for the reduction potentials turned out to be less negative, and the rearrangement energies suffered a significant reduction, as shown in Table 2.

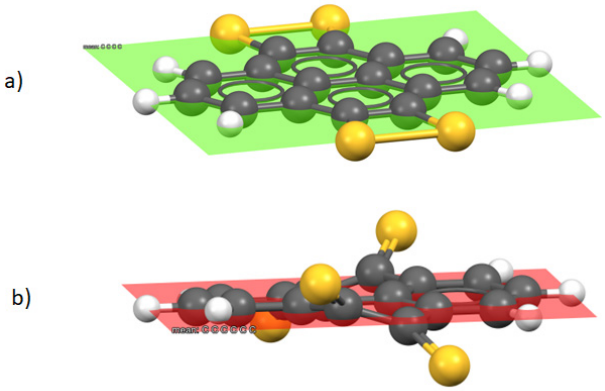

Figure 4. Conformers of compound PTS, (**a**) sulfur atoms coplanar to the ring, (**b**) sulfur atoms out of the plane of the carbon skeleton.

This new spatial arrangement for PTS also influenced the energy of the orbitals involved in the transfer of electrons in LUMO + 1, LUMO and HOMO, which are indicated comparatively in Figure 5. This fundamentally affects the energy of the neutral molecule and the monoanion. Thus, for the neutral molecule, the energy difference was clear for the three orbitals (LUMO + 1, LUMO and HOMO, 0.53 eV, 0.72 eV and 0.52 eV) and decreased for the monoanion (LUMO + 1, LUMO and HOMO, 0.10 eV, 0.28 eV and 0.28 eV). For the di-, tri- and tetra-anion, this difference decreased almost completely since, with the gain of electrons, the sulfur atoms moved to the plane of the pyrene rings.

Figure 5. Schematic plot of the HOMO, LUMO and LUMO + 1 orbital energies for the conformers of PTS with planar sulfur (p) and out-of-plane sulfur (oop) in the, −1, −2, −3 and −4 species.

3. Conclusions

The computational results obtained highlight that pyrene-4,5,9,10-tetrathione is a suitable candidate for further experimental studies verifying its suitability as a material for electrodes in batteries, since although pyrene-4,5,9,10-tetraselenone and pyrene-4,5,9,10-tetratellurone present better prospects than 4,5,9,10-tetraoxopyrene, they require the im-

provement of available synthetic techniques or even the discovery of new ones. Meanwhile, plenty of methods for the thionation of carbonyl compounds are available in the literature [14].

Author Contributions: Conceptualization, M.P.V.-T. and J.A.S.; methodology, M.P.V.-T. and J.A.S.; data curation, F.M., F.F., J.V.T., M.P.V.-T. and J.A.S.; writing—original draft preparation, F.M., F.F., J.V.T., M.P.V.-T.. and J.A.S.;. writing—review and editing, J.V.T., M.P.V.-T. and J.A.S.; funding acquisition, F.M., F.F., J.V.T., M.P.V.-T. and J.A.S. All authors have read and agreed to the published version of the manuscript.

Funding: This work was funded by the Ministerio de Ciencia y Tecnología, Spain (Project MAT201786109P).

Institutional Review Board Statement: Not applicable.

Informed Consent Statement: Not applicable.

Data Availability Statement: Not applicable.

Acknowledgments: Galicia Supercomputing Centrer (CESGA) for computing facilities.

Conflicts of Interest: The authors declare no conflict of interest.

References

1. Miao, L.; Liu, L.; Shang, Z.; Li, Y.; Lu, Y.; Cheng, F.; Chen, J. The structure–electrochemical property relationship of quinone electrodes for lithium-ion batteries. *Phys. Chem. Chem. Phys.* **2018**, *20*, 13478–13484. [CrossRef]
2. Armand, M.; Tarascon, J.M. Building better batteries. *Nature* **2008**, *451*, 652–657. [CrossRef] [PubMed]
3. Lyu, H.; Sun, X.G.; Dai, S. Organic Cathode Materials for Lithium-Ion Batteries: Past, Present, and Future. *Adv. Energy Sustainability Res.* **2021**, *2*, 2000044. [CrossRef]
4. Zhu, Z.; Hong, M.; Guo, D.; Shi, J.; Tao, Z.; Chen, J. All-Solid-State Lithium Organic Battery with Composite Polymer Electrolyte and Pillar [5]quinone Cathode. *J. Am. Chem. Soc.* **2014**, *136*, 16461–16464. [CrossRef] [PubMed]
5. Zhang, M.; Zhang, Y.; Huang, W.; Zhang, Q. Recent Progress in Calix[n]quinone (n = 4, 6) and Pillar [5]quinone Electrodes for Secondary Rechargeable Batteries. *Batter. Supercaps* **2020**, *3*, 476–487. [CrossRef]
6. Yoo, G.; Pyo, S.; Gong, Y.J.; Cho, J.; Kim, H.; Kim, Y.S.; Yoo, J.J.C. Highly reliable quinone-based cathodes and cellulose nanofiber separators: Toward eco-friendly organic lithium batteries. *Cellulose* **2020**, *27*, 6707–6717. [CrossRef]
7. Shi, J.L.; Xiang, S.Q.; Su, D.J.; He, R.X.; Zhao, L.B. Revealing practical specific capacity and carbonyl utilization of multi-carbonyl compounds for organic cathode materials. *Phys. Chem. Chem. Phys.* **2021**, *23*, 13159–13169. [CrossRef] [PubMed]
8. Frisch, M.J.; Trucks, G.W.; Schlegel, H.B.; Scuseria, G.E.; Robb, M.A.; Cheeseman, J.R.; Scalmani, G.; Barone, V.; Petersson, G.A.; Nakatsuji, H.; et al. *Gaussian 16, Revision C.01*; Gaussian, Inc.: Wallingford, CT, USA, 2016.
9. Wang, M.; Dong, X.; Escobar, I.C.; Cheng, Y.-T. Lithium Ion Battery Electrodes Made Using Dimethyl Sulfoxide(DMSO) A Green Solvent. *ACS Sustain. Chem. Eng.* **2020**, *8*, 11046–11051. [CrossRef]
10. Wang, D.; Huang, S.-P.; Wang, C.; Yue, Y.; Zhang, Q.-S. Computational Prediction for Oxidation and Reduction Potentials of Organic Molecules Used in Organic Light-Emitting Diodes. *Org. Electron.* **2019**, *64*, 216–222. [CrossRef]
11. Shoaib, M.; Bibi, S.; Ullah, I.; Jamil, S.; Iqbal, J.; Alam, A.; Saeed, U.; Bai, F.Q. Theoretical Investigation of Perylene Diimide derivatives as Acceptors to Match with Benzodithiophene based Donors for Organic Photovoltaic Devices. *Z. Phys. Chem.* **2021**, *235*, 427–449. [CrossRef]
12. Ji, L.-F.; Fan, J.-X.; Zhang, S.-F.; Ren, A.-M. Theoretical investigations into the charge transfer properties of thiophene α-substituted naphthodithiophene diimides: Excellent n-channel and ambipolar organic semiconductors. *Phys. Chem. Chem. Phys.* **2017**, *19*, 13978–13993. [CrossRef] [PubMed]
13. Evans, D.H. One-Electron and Two-Electron Transfers in Electrochemistry and Homogeneous Solution Reactions. *Chem. Rev.* **2008**, *108*, 2113–2144. [CrossRef] [PubMed]
14. Organic Chemistry Portal. Available online: https://www.organic-chemistry.org/synthesis/C2S/thioketones.shtm (accessed on 17 October 2022).